Experimental Investigation of Transient Voltage and Current Characteristics on a Grounding Mesh

A. Ametani[1], N. Nagaoka[1], T. Sonoda[2], S. Sekioka[3]

(1) Doshisha University, (2) Kansai Electric Power, (3) Kansai Tec.

***Abstract* – This paper investigates transient voltage and current characteristics on a grounding mesh based on field measurements. The grounding mesh is composed of a number of hard copper wires (HDCC 60mm^2) with the maximum length of 34.1m and the maximum width of 24.8m and is buried at the depth of 1m from the ground surface. A current from a pulse generator (PG) and from an impulse voltage generator (IG) is applied at various positions of the mesh to observe transient voltage and current distributions on the mesh. A weather-proof mobile IG with the maximum output voltage of 3MV and the current of 40kA is used to investigate a nonlinear characteristic on the mesh. It is observed in the measured results that the propagation velocity and the attenuation along a buried naked conductor is significantly different from those of a current. A transient grounding impedance of a single counterpoise shows current-dependence which becomes less noticeable as the counterpoise length becomes longer. Voltage and current distributions on a mesh are dependent on the current applied node, and a transient grounding impedance of a mesh shows a polarity effect, and decreases as the applied current increases.**

Keywords – grounding mesh, grounding impedance, wave propagation, nonlinearity, transient

I. Introduction

Electromagnetic disturbance of a low voltage control circuit in a power station and a substation is becoming an important problem as a number of digital circuits composed of sensitive semiconductors have been adopted in the control circuit. In fact, a few disturbances have been experienced in Japan [1-3]. During 10 years since 1989, 307 cases of the disturbances in the control circuit are informed, and about 70% (220 cases) is estimated due to lightning. Among the 220 cases, 104 cases are of the voltage class 66-77kV, 45 cases/110-154kV, 14 cases above 154kV, and 57 cases the voltage class unknown. The incoming path of a lightning surge causing the disturbances has been investigated in the hydraulic generator stations and substations, and the result indicates two dominant paths : (1) via PDs and CTs from a main circuit, (2) via grounding systems due to arrester operation and etc. from an overhead line and a main circuit. It is statistically found that more than 20% of the lightning surges are coming through the grounding systems, and another 20% through PDs and CTs.

Considering the above, the authors have carried out a series of field measurements of lightning surge propagation on grounding systems [3-6]. This paper presents a measured result of surge propagation on a grounding mesh.

II. Experimental Setup

Fig. 1(a) illustrates an experimental setup of a grounding mesh composed of a hard cupper conductor (HDCC 60mm^2). The mesh is buried at the depth of 1m with the length of x_0 to the x-direction and of y_0 to the y-direction. Three types of the mesh in Fig. 1(b) to (d) are tested. The field measurements were carried out in three different test sites and different time periods to obtain a reliable information. The earth resistivity was measured by Wenner's method (Yokogawa Type 3244) and the following results (averaged) were obtained.

Site 1 : r_e =200 [Ωm], Site 2 : 100-300 , Site 3 : 300

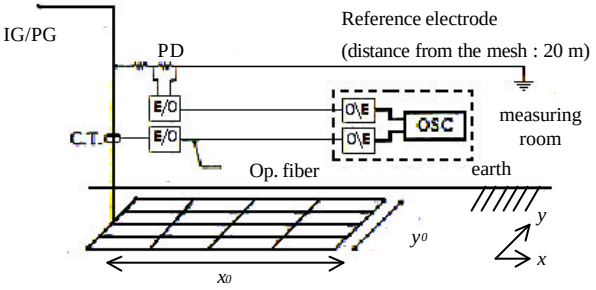

(a) Experimental setup

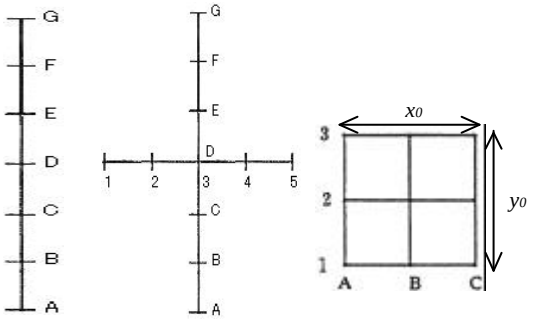

(b) Single (c) Cross-shaped (d) Mesh-I

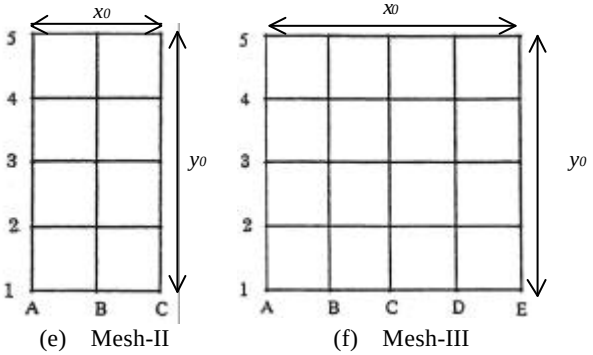

(e) Mesh-II (f) Mesh-III

Fig. 1 Experimental setup

A current with the maximum amplitude of about 2A is applied from a pulse generator (PG) to various nodes (center, corner and etc.) of a mesh. Currents and voltages are measured at various nodes of the mesh. In the case of heavy current application, a mobile impulse voltage generator (IG) with the maximum voltage 3MV and current 40kA is used [7]. A voltage is measured via a resistive divider (20kΩ, rise time 80ns), and a current is measured via a Peason CT (Model-110A, rise time 100ns) by using an oscilloscope (Tektronix TDS540, sampling frequency 500MHz).

A PG application is to observe a linear characteristic of wave propagation on a grounding mesh, and an IG application is to observe a nonlinearity of the wave propagation.

III. Basic Propagation Characteristics on a Buried Naked Conductor (Counterpoise)

A. Single Straight Conductor (Fig. 1(b))

i) Linear characteristic (PG application)

Fig. 2 summarizes the propagation velocity and attenuation of voltage and current traveling waves evaluated from the measured waveforms at Sites 1 and 3 [8]. The velocity is determined by the arrival time at a node from a reference node (voltage/current applied node). The attenuation is defined as the ratio of the peak values at the sending end (node A, x=0) and node k (k=B to E, i.e. x=5 to 30m). It should be noted that the earth resistivity is not the same in the measurements at the Test Sites 1 to 3. It is clear in the figure that the propagation velocity and the current peak decreases as the distance increases. The voltage peak decreases up to a certain distance and then stays constant. The observation indicates that the counterpoise is not uniform nor homogeneous.

ii) Nonlinear characteristic (IG application)

Fig. 3 shows a measured result of voltage and current attenuation on a conductor with the total length x_0=30m, when a current of 10.64kA from the IG is applied. It is observed from voltage and current waveforms that the time to peak of the current is nearly independent from the distance from the sending end, while that of the voltage increases noticeably as the distance increases. On the contrary, the current peak decreases significantly as the distance increases, while the voltage peak decreases by about 20% upto node D (x=15m) and then stays constant as observed in Fig. 3. A comparison of Fig. 3 with Fig. 2 indicates that the voltage attenuation is far smaller in the heavy current (IG, 10.64 kA) case than that in the small current (PG, 0.2-1A) case, while the current attenuation is nearly the same in the both cases although the earth resistivity is not the same in the measurements.

Fig. 4 shows the current and voltage peak values normalized by those at the sending end as a function of the applied current. The currents along the conductor tend to increase, while the voltages tend to decrease as the applied current increases. In other words, the attenuation of the currents and the voltages on a counterpoise are current-dependent nonlinear. Also, the grounding impedance (Vmax/Imax) is nonlinear for Fig. 4(b) is equivalent to the impedance.

B. Cross-Shaped Conductor (Fig. 1(c))

Measurements were carried out in Site 2 (r_e =100 to 300 Ωm) with the total length x_0=30m (node A to G) and y_0=20m (node 1 to 5, node 3=node D). The grounding resistance (Vac/Iac) of the cross-shaped counterpoise is measured to be 12.2Ω, while that of a single one (node A to G) is about 20Ω as shown in Fig. 5.

i) PG Application

Fig. 6 shows a comparison of current and voltage waveforms on the single (-) and the cross-shaped (+) counterpoises, when a current of about 1A is applied to node A. It is observed that there is no difference of the voltage waveform between the two cases until reflection

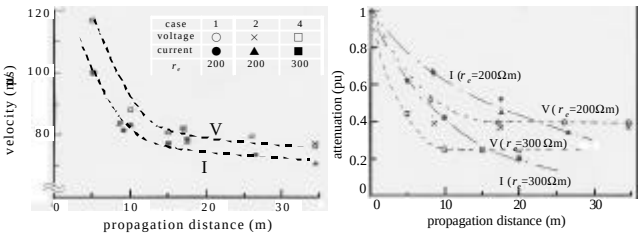

(a) Propagation velocity (b) Attenuation : $f(x)/f(x=0)$

$f(x)$: voltage or current as a function of conductor length

Fig. 2 Propagation velocity and attenuation of voltage and current traveling waves

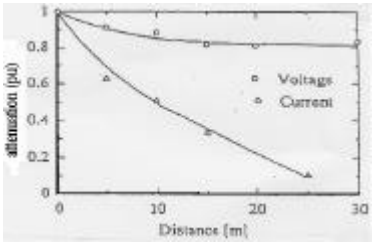

Fig. 3 Attenuation $f(x)/f(x=0)$ for x_0=30m, I_0=10.64kA

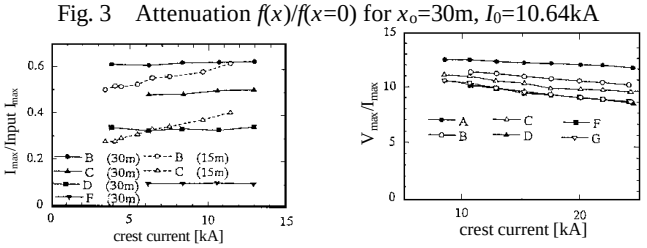

(a) Current (b) Voltage

Fig. 4 Normalized peak values of currents and voltages vs applied current

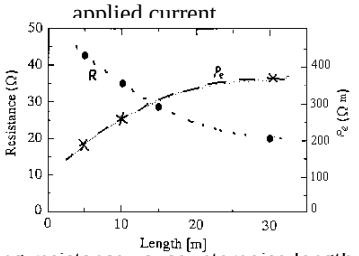

Fig. 5 Grounding resistance vs. counterpoise length in Site 2

from the remote end comes back.. After the reflection, the voltages deviate from each other, and the voltage on the cross-shaped one is smaller by about 25 % than that on the single counterpoise. The difference roughly corresponds to the difference of the grounding resistance between the two cases (+12.2Ω, -20Ω).

ii) IG Application

Fig. 7 shows a grounding impedance ($=V_{max}/I_{max}$) versus applied current characteristic on the cross-shaped counterpoise (+) and on the single counter poise (-) corresponding to Fig. 4(b). It is clear that the resistance of the cross-shaped one, of which the total counterpoise length ($x_0 + y_0$) is greater, is smaller than that of the single one. The impedance at node A in Fig. 7(a) is relatively greater than those at the other nodes. These phenomena correspond to the fact that the current reduction is far greater nearby the current injected node as observed in Fig. 3. In other words, the grounding impedance is significantly affected by the part of a counterpoise nearby the current injected node. It is observed that the current-dependence on the single counterpoise is more noticeable than that on the cross-shaped one in Fig. 7(b). The reason for this is that the distance from the current injected node (node D) to the remote ends (nodes A and G) is small compared with that in Fig. 7(a) and the injected current is distributed to the both sides, i.e. the current to each part (nodes D to A and D to G) is small.

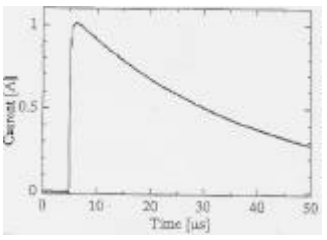

(a) Current at node A

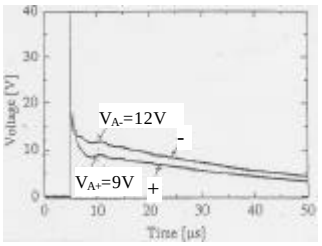

(b) Voltage at node A

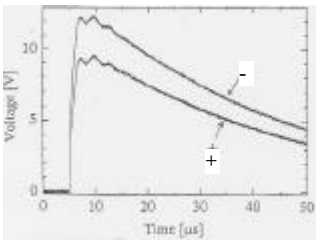

(c) Voltage at node D = node 3

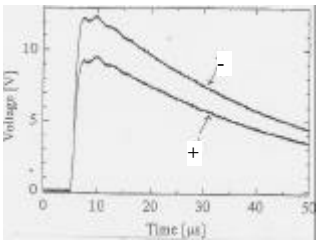

(d) Voltage at node G

Fig. 6 Current and voltage waveforms on a single (-) and a cross-shaped counterpoise

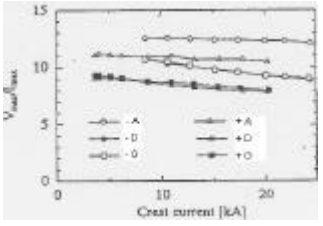

(a) Node A application

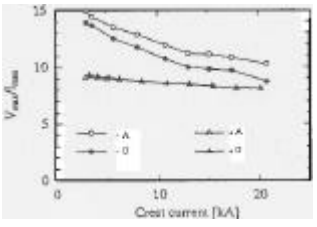

(b) Node D application

Fig. 7 Grounding impedance vs. applied current

IV. Transient Voltage and Current on a Grounding Mesh with PG Application

A. Mesh —I and II

Fig. 8(a) shows measured waveforms of transient voltages and currents at various nodes and branches of the mesh-I (square shape : $x_0 = y_0 = 10$ m) when a current from a PG is applied to the mesh corner, i.e. node A1 in Site 3, and (b) shows those of the mesh-II (rectangular shape : x_0 =10m, $y_0 = 20$ m). It is observed that the initial part of the waveforms in Fig. 8(a) is the same as that in Fig. 8(b), because the geometrical configuration is the same upto nodes C and 3. The last part of voltage in (b) is smaller than that in (a). On the contrary, the current waveforms in Fig. 8(a) and (b) are nearly the same. As a result, the transient grounding impedance of the mesh-II becomes smaller than that of the mesh-I. The result is reasonable, for the grounding impedance is expected to be inversely proportional to the area of the mesh. The transient impedance (time dependence) seen from the current injected node clearly show an inductive nature.

The current distribution on the mesh-I is nearly symmetrical for the geometrical symmetry of the mesh, while that on the mesh-II is asymmetrical.

B. Mesh —III

Fig. 9 shows transient current waveforms on various branches of the mesh-III (x_0 =34.1m, y_0 =24.8m), when a current from the PG is applied to (a) Node A (mesh center), (b) Node B and (c) Node C (the nearest corner to the PC). The current distribution is observed to be not symmetrical due to the distance to the current applied node and the asymmetry of the branches to the PG. For example, $I(\mathrm{A}-4) > I(\mathrm{A}-3) > I(\mathrm{A}-1) > I(\mathrm{A}-2)$ corresponding to the distance $\mathrm{A}-4 < \mathrm{A}-3 < \mathrm{A}-1 < \mathrm{A}-2$ to the PG. The propagation velocity of the current in Fig. 9(a) is

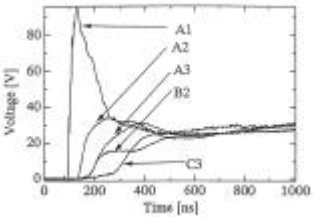

(1) Voltage

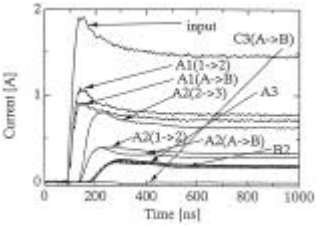

(2) Current

(a) Mesh-I (Square)

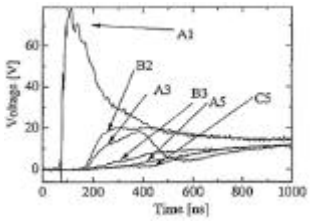

(1) Voltage

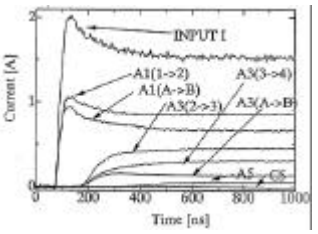

(2) Current

(b) Mesh-II (Rectangular)

Fig. 8 Transient voltage and current waveforms

estimated to be 95.4m/μs on the branch $A-5$ and $A-7$ (distance from Node A : 12.4m), and 85.3m/μs on the branch $A-6$ (17.05m).

Fig. 10 shows transient voltages at various nodes. A comparison with Fig. 8 clearly shows more sharp rise and less amplitude at the wavefront of the voltage at the current applied node in Fig. 10 due to a smaller impedance of the mesh-III. Fig. 10(c) summarizes the amplitude at the wavefront for PG application to various nodes. It is clear that the Node A application gives the highest voltage at the applied node, i.e. the highest impedance of the grounding mesh seen from the applied node for the applied current is the same in each case, and the Node B application gives the lowest voltage and the lowest impedance. In general,

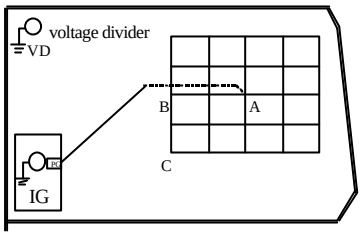

Distance VD to B = 20 m
IG to B = 15 m

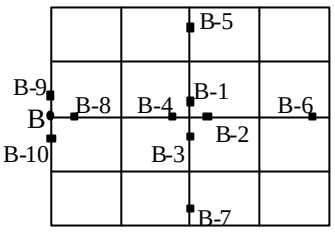

(1) Circuit diagram

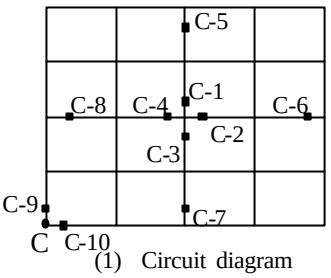

(1) Circuit diagram

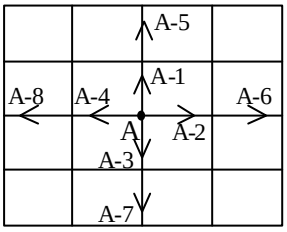

(1) Circuit diagram

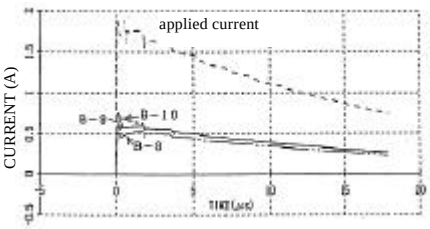

(2) Applied current and branches B-8 to B-10

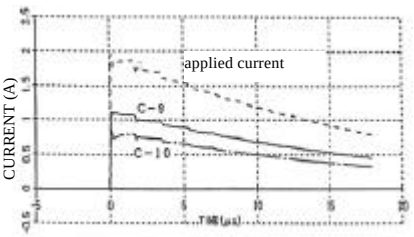

(2) Applied current and branches C-9, C-10

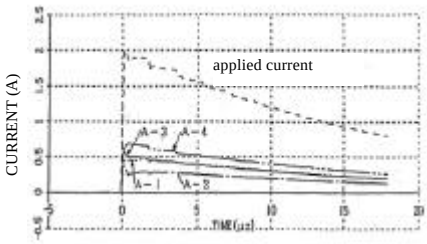

(2) Applied current and branches A-1 to A-4

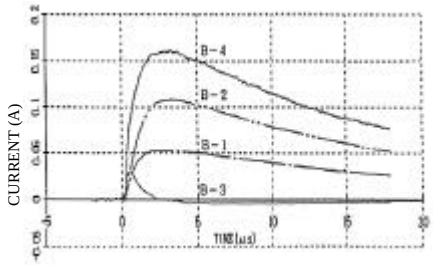

(3) Branches B-1 to B-4

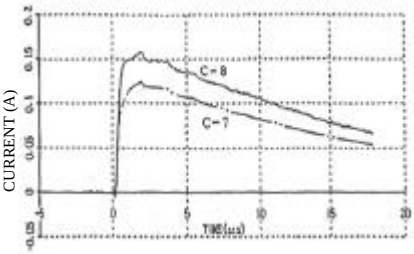

(3) Branches C-7, C-8

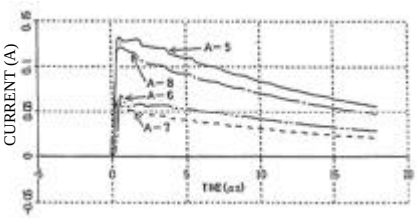

(3) Branches A-5 to A-8

(a) Node A application

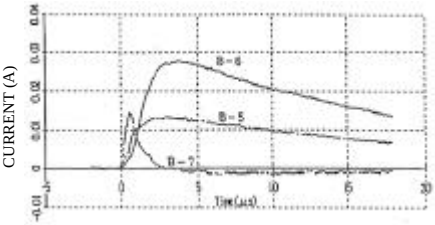

(4) Branches B-5 to B-7

(b) Node B application

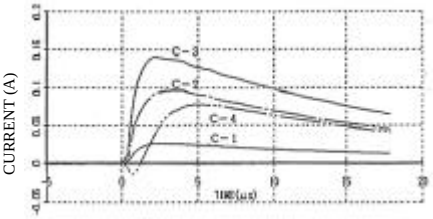

(4) Branches C-1 to C-4

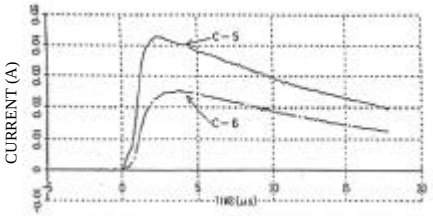

(5) Branches C-5, C-6

(c) Node C application

Fig. 9 Transient currents

the mesh impedance becomes lower as the number of connected branches to the current applied node increases.However, Fig. 10 dose not follow the theory. The reason for this is estimated to be the induction effect from a current lead wire and a voltage reference wire.

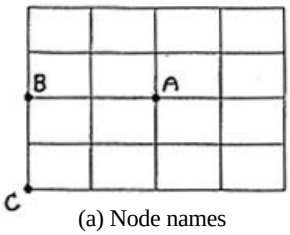

(a) Node names

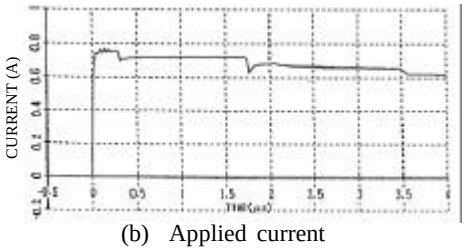

(b) Applied current

PG applied node	measured node		
	A	B	C
A	47.9	2.7	3.2
B	2.3	27.6	3.7
C	2.8	4.4	36.8

(c) Maximum voltage

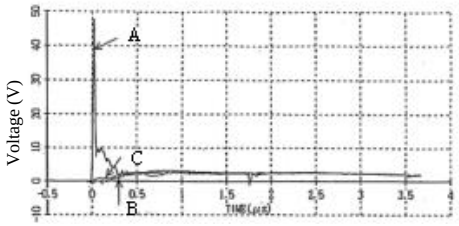

(d) Node A application

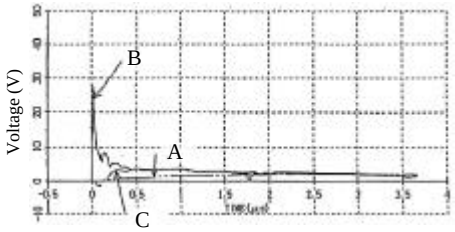

(e) Node B application

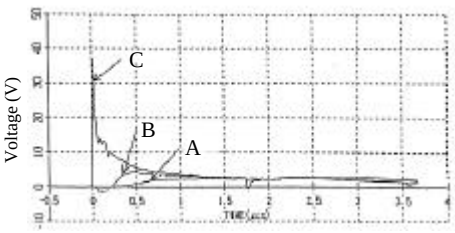

(f) Node C application

Fig. 10 Transient voltages

V. GROUNDING IMPEDANCE OF MESH

A. Steady-State Resistance (PG Application)

Table 1 shows a steady-state resistances of the grounding mesh-I and mesh-III measured on three different days to obtain reliable data.

It is observed in the table that the resistance is inversely proportional to the area S of a grounding mesh, i.e. R_I (=14~19Ω)/ R_{III} (=5.6~7.4Ω) ≈ 2.5= S_{III} (=20×20)/ S_I (= 10×10), corresponding to a well-known formula of the resistance, i.e.

$$R = r / S$$

where r : resistivity [Ω•m], S : cross-section area [m^2]

Table 1 Steady-state resistance of grounding meshes

date	resistance [Ω]		earth resistivity
in 1998	mesh-Ⅰ (10×10m)	mesh-Ⅲ (20×20m)	[Ω·m]
11 Sept.	19	7.4	359
22 Oct.	14.2	5.6	295
30 Dec.	———	5.9	339

B. Current-Dependent Impedance (IG Application)

Fig. 11 shows a current-dependent impedance of the grounding mesh-III (34.1×24.8m) when a current from the IG is applied to (a) Node A and (b) Node B. The impedance decreases as the current increases. It should be noted that the Node B application shows a higher impedance as expected, contrary to the observation in Fig. 10. The polarity affect is not observed in Fig. 11(b).

Fig. 12 shows another measured result of a current-dependent impedance for various meshes and current application nodes. From the figure, the following observations are made.

(1) The impedance in the case of center (Node A) application is smaller than that in the corner (Node B) application.

(2) The ratio of the impedances in the cases of the center and the corner application is about 0.9 in the mesh-I and is 0.5 to 0.6 in the mesh-III.

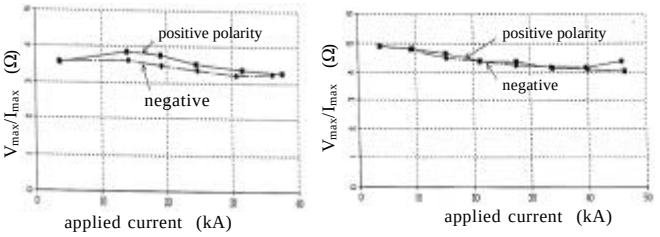

(a) Node A application (b) Node B application

Fig. 11 Current-dependent impedance of mesh-III

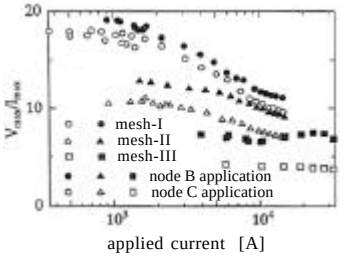

Fig. 12 Current-dependent impedance of various meshes

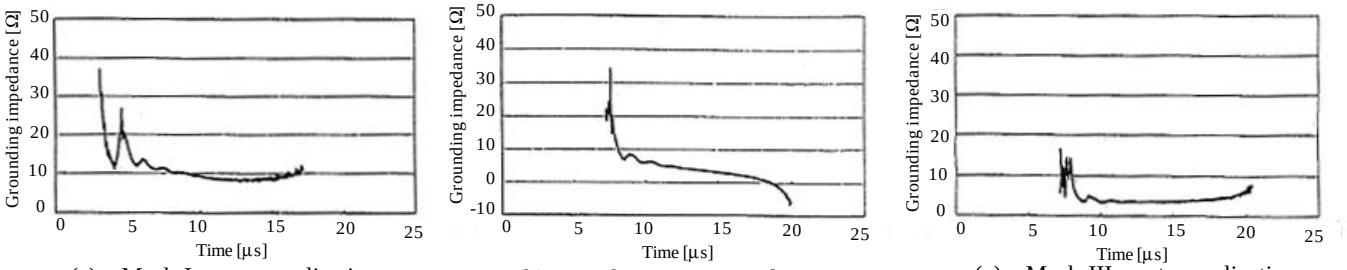

Fig. 13 Transient response of grounding impedance

The impedance of the mesh-I decreases inversely proportional to the applied current above 1kA, while that of the mesh-III is nearly constant independently from the applied current. This fact indicates that the current-dependence (nonlinearity) of the mesh grounding impedance is significantly dependent on the mesh area, i.e. the smaller the area, the greater the nonlinearity.

The nonlinear current-dependent characteristic of the grounding impedance is estimated to be caused by soil ionization due to a heavy current [5]. As the current increases, the soil ionization increases and the apparent radius of the mesh conductor becomes greater. Thus, the grounding impedance decreases.

C. Transient Response of Grounding Impedance (IG Application)

Fig. 13 shows a transient response of the grounding impedance of the mesh-I (10×10^{m}) and the mesh-III (20×20^{m}), when an impulse voltage of about 150 to 160kV from the IG is applied to the corner and the center of the meshes. The transient response is defined by

$Z(t)$ [Ω]=voltage $v(t)$ at the applied node [V] /
applied current $i(t)$ [A]

Similarly to a rod electrode, the impedance of a grounding mesh shows a transient characteristic. The impedance in Fig. 13 shows an inductive nature and the peak value is about 3 to 4 times of the steady-state value. The impedance in the case of the corner application shows a sharper rise at the beginning and a greater value in comparison with the case of the center application.

VI. CONCLUSIONS

Based on the measured results of transient voltages and currents on grounding systems, the following conclusions have been obtained.

(1) The propagation velocity and the attenuation of a voltage traveling wave along a buried naked conductor (counterpoise) are significantly different from those of a current traveling wave.

(2) A transient grounding impedance of a single counterpoise shows current-dependence which becomes less noticeable as the counterpoise length becomes longer. The current-dependence of a cross-shaped counterpoise composed of two counterpoises is less noticeable than that of the singles counterpoise.

(3) Voltage and current distributions on a grounding mesh and the grounding impedance are dependent on the current applied node, the geometrical configuration and the area of the grounding mesh. The rise time and the amplitude of the transient voltage waveform becomes smaller as the mesh area becomes greater. Correspondingly, the grounding impedance decreases.

(4) The transient grounding impedance shows an inductive nature, and the peak value is about 3 to 4 times of the steady-state value.

(5) The grounding impedance is current-dependent. When the mesh area is small, the impedance decreases inversely propotional to the applied current. If the mesh area is large, the current-dependence is less noticeable.

REFERENCES

[1] T. Hasegawa, et.al., A fact-finding analysis of lightning disturbances of low-voltage control circuits in power stations and substations, IEE of Japan, Annual Meeting Records, Paper 1218, 1992

[2] "Technologies of Countermeasures against Surges on Protection Relay and Control Systems", Report of Japanese ETRA, vol. 57, No. 3, Jan. 2002

[3] T. Sonoda, et.al., An experimental study on surges induced from grounding grid to low-voltage control circuits, IEE of Japan, Research Meeting, Paper HV-01-129, 2001

[4] S. Yamaguchi, et.al., Surge characteristics of a counterpoise, IEE of Japan, Research Meeting, Paper HV-97-88, 1997

[5] S. Sekioka, et. al., Measurements of grounding resistances for high impulse currents, IEE Proc. -GTD, vol. 145(6), pp. 693-699, 1998

[6] T. Sonoda, et.al., Impulse characteristics of grounding resistance of counterpoise, Trans. IEE of Japan, vol. 121-B(5), pp. 671-676, 2001

[7] A. Morimoto, et.al., Development of all-weather-type mobile impulse voltage generator and its application to experiments on nonlinearity of grounding resistance, Trans. IEE of Japan, vol. B-117(5), pp. 22-33, 1995

[8] A. Ametani, et.al. : Basic investigation of wave propagation characteristics on an underground naked conductor, Proceedings of ICEE '02, Jeju (Korea), pp. 2141-2146, 2002